

Photocatalytic H₂ generation using dewetted Pt-decorated TiO₂ nanotubes – Optimized dewetting and oxide crystallization by a multiple annealing process

by JeongEun Yoo,^{1†} Marco Altomare,^{1†} Mohamed Mokhtar,² Abdelmohsen Alshehri,² Shaeel A. Al-Thabaiti,² Anca Mazare,¹ and Patrik Schmuki^{1,2*}

1 Department of Materials Science, Institute for Surface Science and Corrosion WW4-LKO, Friedrich-Alexander University, Martensstraße 7, D-91058 Erlangen, Germany

2 Chemistry Department, Faculty of Sciences, King Abdulaziz University, 80203 Jeddah, Saudi Arabia Kingdom

† These authors contributed equally

* Corresponding author. E-mail: schmuki@ww.uni-erlangen.de, Tel.: +49-9131-852-7575, Fax: +49-9131-852-7582

This document is the unedited Author's version of a Submitted Work that was subsequently accepted for publication in *The Journal of Physical Chemistry C*, copyright © American Chemical Society after peer review.

To access the final edited and published work see:

<http://pubs.acs.org/doi/abs/10.1021/acs.jpcc.5b12050>

DOI: 10.1021/acs.jpcc.5b12050

ABSTRACT

In the present work we use TiO₂ nanotube arrays, carrying a Pt coating that is optimally dewetted, as a photocatalyst to generate H₂. In order to achieve a maximum H₂-generation efficiency, on the one hand an ideal thermal dewetting of the Pt layer into nanoparticles is needed that requires an oxygen free heat treatment, and on the other hand an optimal crystallization of the TiO₂ nanotubes into anatase with reduced defect density is achieved only by annealing in O₂ containing environment. To overcome this issue, we combine adequate reducing and oxidizing conditions in a multiple annealing treatment, and obtain Pt-decorated anatase TiO₂ nanotubes showing significantly enhanced photocatalytic H₂ generation ability.

INTRODUCTION

Since the groundbreaking work of Fujishima and Honda,¹ the generation of H₂ through photocatalytic water splitting on semiconductors has been widely investigated, as it is perceived as a most promising way for the sustainable generation of energy. A photocatalytic process is in general based on light absorption by a semiconductor that leads to charge carrier generation: electrons are photopromoted to the conduction band, while holes are left in the valence band. Electrons and holes on the respective bands may then migrate to the semiconductor surface and induce red-ox reactions with species in the environment.²⁻⁴

Among the different photocatalytic materials that have been developed in the last decades, TiO₂ still represents one of the most promising semiconductor metal oxides, being cheap, non-toxic, (photo-)chemically stable and, most importantly, having suitable band edge positions. For anatase TiO₂, the conduction band edge lies at ca. -0.25 V (vs. SHE, pH 1)^{5,6} – the conduction

band electrons are thus thermodynamically able to reduce water into H₂. Nevertheless, this reaction is not only hampered by charge carrier recombination and trapping phenomena, but also by the sluggish kinetics of electron transfer to the environment.⁷ These issues can be tackled by i) nanostructuring the semiconductor,^{8,9} and by ii) using suitable co-catalysts (mostly Pt, Pd and Au).¹⁰⁻¹⁴

When nanostructured TiO₂ is used as photocatalyst, the charge carriers have to migrate only over relatively short distances (nm-scale) to reach the surface and react with the environment, and this reduces the probability of charge carrier recombination and trapping.¹⁵ Among several approaches to fabricate nanostructures,^{8,16-18} electrochemical anodization of metallic Ti, that leads under self-organizing conditions to highly-ordered and vertically aligned TiO₂ nanotubes (NTs),^{19,20} is one of the most facile techniques. A key advantage of this approach is that the structural properties of the nanotubes (wall thickness, tube diameter and length, etc.) can be easily tailored simply by the electrochemical conditions (e.g., adjusting applied voltage, water and fluoride contents).^{21,22}

The second typical measure to increase the efficiency of TiO₂ photocatalysts is the deposition of noble metal co-catalysts, such as Au, Pd or Pt, onto its surface. These co-catalysts not only act as “electron sink” (i.e., by trapping conduction band electrons),^{23,24} but also enable efficient electron transfer to the environment.⁶

Recently we reported on a most straightforward way to decorate TiO₂ nanotube layers with co-catalyst particles that is to first coat the tubes with a thin sputter-deposited film of the noble metal (Au, Pt) and then to thermally dewet this thin film to particles,²⁵⁻²⁸ i.e., a suitable thermal treatment breaks up the metal film into small particles.²⁹ Dewetting of thin Au films on TiO₂ can

be achieved by a simple annealing in air at 450°C. These annealing conditions are ideal as they also lead to crystallization of the TiO₂ tubular substrate (that after formation is amorphous) into anatase which is the most photocatalytically active TiO₂ polymorph. In other words, a single step annealing can at the same time be used to crystallize TiO₂ to anatase and induce Au dewetting.

While this air treatment is ideal for Au, for Pt (an even more effective co-catalyst)²³ the situation is different. A main issue of Pt is that dewetting on TiO₂ substrates normally requires relatively higher temperatures ($T \geq 500^\circ\text{C}$) and must be carried out in Ar or N₂ atmosphere (one of the main reasons is that the occurrence of Pt oxide^{30,31} interferes with dewetting and leads to significant photoactivity decay).³² On the other hand annealing in such a reductive atmosphere leads to a partial reduction of TiO₂ – these reduced states lead in general to charge carrier trapping and recombination.³³

In this work we try to overcome this issue by combining reducing and oxidizing annealing treatments. We show that optimized annealing can lead to a drastically increased photocatalytic efficiency in terms of a maximized H₂ evolution efficiency.

EXPERIMENTAL

Ti foils (0.125 mm thick, 99.7% purity, Goodfellow, England) were degreased by sonicating in acetone, ethanol, deionized water, and then dried in a N₂ stream. The Ti foils were then anodized to fabricate the highly ordered TiO₂ nanotubes arrays in an electrolyte based on o-H₃PO₄ with 3 M HF (Sigma-Aldrich).²⁵ For the anodic growth, a two-electrode configuration was used, where the Ti foil and a Pt gauze were the working and counter electrodes, respectively. The anodization experiments were carried out applying a potential of 15 V (for 2 h) provided by a Volcraft VLP

24 Pro DC power supply. After the anodization, the nanotube films were rinsed with ethanol and dried in a N₂ stream.

The tube oxide layers, either as-formed (i.e., amorphous) or thermally treated, were coated by thin Pt films with a nominal thickness in the range of 1-15 nm.

The tubes were exposed to different thermal treatments. Annealing in ambient air was carried out at different temperatures (350-550°C) for 1 h, using a Rapid Thermal Annealer (Jipelec Jetfirst 100 RTA), with a heating and cooling rate of 30°C min⁻¹. Annealing in pure O₂ (99.95 %, Linde) was carried out at 450°C for 30 min, in a VMK80S Linn High Therm tubular furnace. The O₂ flux was set to 100 mL min⁻¹. Annealing in pure N₂ (99.999 %, Linde) was carried out at 600°C for 1 h, in a ZEW 1041-5 Heraeus tubular furnace. The N₂ flux was set to 20 NL min⁻¹.

The deposition of Pt on the anodic TiO₂ films was carried out using a high vacuum sputter coater (Leica – EM SCD500). The pressure of the sputtering chamber was reduced to 10⁻⁴ mbar, and then set at 10⁻² mbar of Ar. The applied current was 15 mA. The amount of sputtered Pt was determined by an automated quartz crystal film-thickness monitor.

For morphological characterization, a field-emission scanning electron microscope (Hitachi FE-SEM S4800) was used. X-ray diffraction analysis (XRD, X'pert Philips MPD with a Panalytical X'celerator detector) using graphite monochromized Cu K α radiation (wavelength 1.54056 Å) was used for determining the crystallographic composition of the samples.

The composition and the chemical state of the films were characterized using X-ray photoelectron spectroscopy (XPS, PHI 5600, US), and the spectra were shifted in relation to the C1s signal at 284.8 eV (Pt4f peaks were fitted with Multipak software).

The photocatalytic H₂ generation experiments were carried out by irradiating the oxide films with UV light (HeCd laser, Kimmon, Japan; $\lambda = 325$ nm, expanded beam size = 0.785 cm², nominal power of 60 mW cm⁻²) in a 20 vol% ethanol–water solution (for 9 h) in a quartz tube. The amount of produced H₂ (which accumulated over time within the tube) was measured at the end of the experiments by using a gas chromatograph (GCMSQO2010SE, Shimadzu) equipped with a thermal conductivity detector and a Restek micropacked Shin Carbon ST column (2 m × 0.53 mm). GC measurements were carried out at a temperature of the oven of 45°C (isothermal conditions), with the temperature of the injector set at 280°C and that of the TCD fixed at 260°C. The flow rate of the carrier gas, i.e., argon, was 14.3 mL min⁻¹. Before the photocatalytic experiments, the reactor and the water-ethanol mixtures were purged with N₂ for 30 min to remove O₂. This is strictly needed as O₂ would diminish the efficiency of H₂ generation by competitively undergoing photocatalytic reduction to O^{2•-} (i.e., O₂, instead of water or ethanol, is reduced by conduction band electrons).^{3,34} The photocatalytic experiments were carried out in ethanol–water solution since the presence of specific amounts of organics significantly triggers the H₂ generation. Ethanol acts in fact as a hole-scavenger, that is, the organic molecules are quickly oxidized towards several intermediates and eventually to CO₂. As a result of the fast hole-consumption, conduction band electrons are more readily available for the H₂ generation reaction.³⁵

RESULTS AND DISCUSSION

Fig. 1 shows the morphological features of the short-aspect anodic TiO₂ nanotube layers used in this work. The nanotubes are almost ideally hexagonally packed and have average diameter and

length of 70-80 nm and 150-170 nm, respectively.²⁵ Fig. 1 (b,c) show morphology of the tube substrates after sputter-coating the tubes with a layer of Pt with a nominal thickness of 5 nm. The profile of the noble metal deposition is particularly clear in Fig. 1 (c), where one can see that the Pt film preferentially coats the tube top, and the thickness decreases gradually toward the bottom of the cavities.

The thin Pt films present on the tube substrates can be split up into arrays of fine particles by a thermal treatment at 600°C in N₂ atmosphere for 1 h,³⁶ leading to the Pt/TiO₂ structures shown in Fig. 1 (d,e). Here one can see that in the case of 5 nm-thick sputter-coated Pt films, the particles formed by dewetting are globular and have an average diameter of ca. 5-25 nm, with smaller particles at the bottom and bigger aggregates at the top of the tubes. Such a distribution of the nanoparticles (NPs) is in line with the different initial thickness of the Pt film on the tube walls, that is, the size of the dewetted particles strictly depends on the thickness of the metal film and thinner films generally split into small particles, while thicker coatings form large metal islands.²⁹

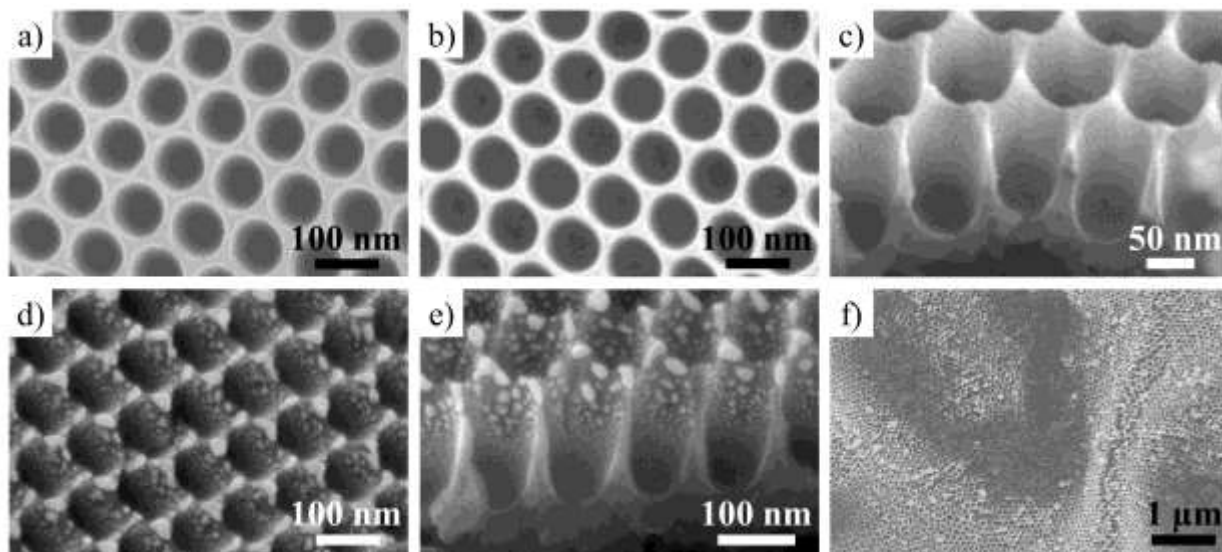


Figure 1. SEM images of TiO₂ nanotube arrays a) as-formed; b) and c) sputter-coated with a 5nm-thick Pt film; d) and e) after thermal dewetting of the Pt film by heat treatment in N₂ at 600°C for 1 h; f) exposed to a thermal treatment in air at 600°C for 1 h.

Noteworthy, only a thermal treatment at 600°C (or higher) in N₂ (or Ar) could lead to defined Pt dewetting onto TiO₂ surfaces while lower temperatures did not affect the morphology of the Pt films even after extended times. A treatment in an O₂-containing atmosphere at 600°C not only leads to partial dewetting of Pt (presumably due to Pt oxide formation) but, even more detrimental, leads also to a complete collapse of the tube structure as shown in Fig. 1 (f). An oxygen treatment at 600°C also leads to extensive growth of thermal titanium oxide from the Ti metal substrate underneath the tubes.^{24,28,37-39}

A first round of photocatalytic experiments showed that Pt dewetting is highly beneficial for the photocatalytic H₂ generation even when this process is carried out in N₂ at 600°C. Dewetted films showed a H₂ production of ~ 20 μL of H₂ / 9h in comparison to non-dewetted layers that

produced $\sim 10 \mu\text{L} / 9\text{h}$, that is, a 100% enhancement can be achieved through the dewetting step.^{25,27}

This result is on the one hand most likely ascribed to the fact that as-sputtered noble metal films coat the TiO_2 tubes in a conformal fashion, and thus shade the underneath structure limiting the absorption of UV light by the semiconductor. On the other side, dewetting forms arrays of Pt nanoparticles homogeneously distributed on the oxide surface and with higher specific area (than a coherent Pt film) that improves the electron transfer to the environment and, as a consequence, the H_2 generation efficiency.²⁶

Nevertheless, Pt-coated tubes annealed in air at 450°C show an even higher H_2 production of $\sim 60 \mu\text{L} / 9\text{h}$, although this thermal treatment does not induce Pt dewetting. This means that an enhanced H_2 evolution must rather be related to a higher quality oxide in the tubes (lower defect density anatase formed by crystallizing in non-reductive conditions).⁴⁰

This clearly indicates that both Pt dewetting (high temperature treatment in N_2) and a suitable crystallization of the oxide (air annealing) are highly beneficial to achieve an enhanced photocatalytic activity. In order to optimize both benefits we explored several annealing conditions of the Pt-coated tubes, at various temperatures and in different atmospheres, and investigated the properties of the films in view of improving their photocatalytic H_2 generation ability.

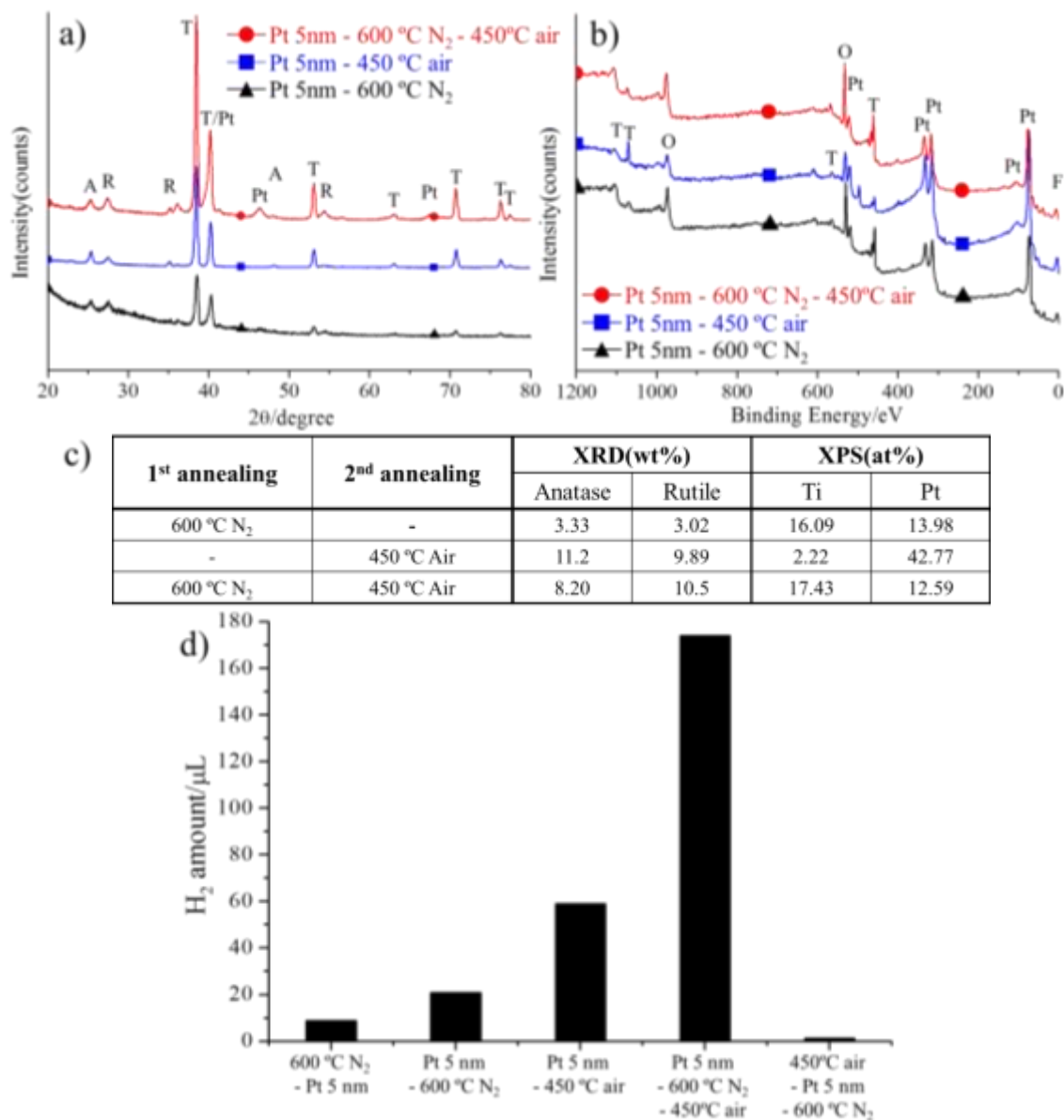


Figure 2. a) XRD patterns, b) XPS surveys c) summary of the XRD and XPS results, and d) photocatalytic H₂ generation results of Pt/TiO₂ nanotube layers exposed to different thermal treatments.

Fig. 2 (a-c) show the XRD and XPS results of differently treated samples. In every case we firstly deposited on the tube layers 5 nm-thick Pt films, and then exposed the layers to different

thermal treatments. From XRD it is evident that for tubular oxides treated in N₂ at 600°C only a relatively low degree of crystallinity is obtained. The content of anatase and rutile TiO₂ phase is only 3.3 and 3.0 wt%, respectively. The low degree of crystallinity can be ascribed to the amorphous nature of as-formed anodic oxides containing a large density of oxygen vacancies – a defect free crystalline material requires annealing in an O₂-containing atmosphere.^{33,41}

In fact by air-annealing at 450°C, the content of anatase and rutile in the oxide films increased up to ca. 11.2 and 9.9 wt%, respectively.⁴² However, as mentioned before, air-annealing does not induce Pt dewetting. Nevertheless, we found that a multiple treatment consisting of N₂-annealing at 600°C followed by air-annealing at 450°C can provide dewetting and leads as well to a relatively high degree of oxide crystallinity, with contents of anatase of ca. 8.2 wt%.

XPS results showed all films to be generally composed of TiO₂ and Pt metal, with a small content of fluorine, most probably due to F-ion uptake by the oxide during the electrochemical growth in the HF electrolyte. Also, from the XPS data the occurrence of Pt dewetting is traceable. The surface Ti amount apparent in XPS for non-dewetted films (air-annealed at 450°C) is relatively low (2.2 at%) while Pt is accordingly high (42.8 at%), confirming that the oxide surface is well coated by the sputtered Pt film. After the films are N₂-treated at 600°C the Ti surface content increased up to 16-17 at%, indicating that Pt agglomerated and thus more open oxide surface becomes detectable.

The Pt/oxide films treated under different annealing conditions were tested as catalysts for H₂ generation from H₂O-ethanol solutions. From the results summarized in Fig. 2 (d) it is clear that the different thermal treatments (different temperatures and atmospheres) have dramatic effects on the H₂ generation efficiency.

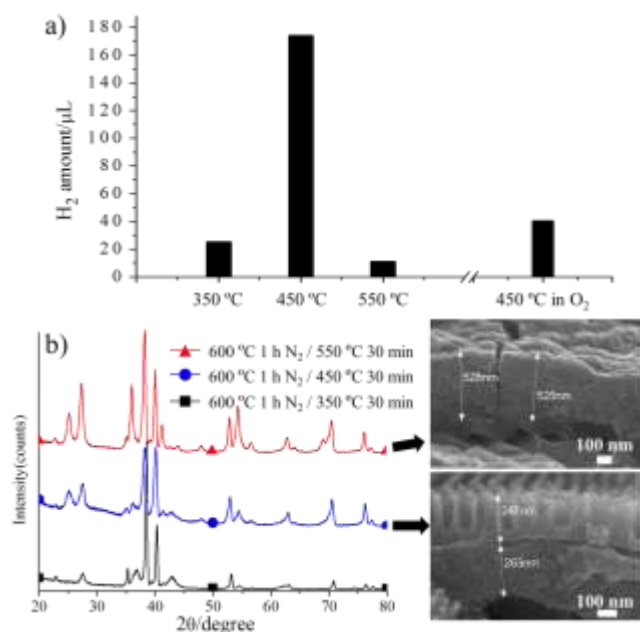


Figure 3. a) Photocatalytic H₂ generation data and b) XRD patterns of TiO₂ nanotube layers decorated with sputter-dewetted particles and exposed to different thermal treatment in O₂-containing environment. The SEM images in b) show the thickness of the rutile under layer formed after air-annealing at 450°C (lower) and 550°C (upper).

In line with the observations above, a first level of photocatalytic enhancement is achieved with the more co-catalytically efficient Pt nanoparticles formed by dewetting (N₂-annealing), compared to a conformal noble metal film (i.e., ~ 20 vs. 10 μL H₂ / 9h). Then, the H₂ generation efficiency is further improved up to ~ 60 μL H₂ / 9h, even without Pt dewetting, by optimizing the quality of the oxide with an air-annealing treatment^{33,43} However, most relevant is that the two concepts can be beneficially combined through a multiple annealing approach, i.e., to provide both Pt dewetting and anatase nanotubes: Pt/tube layers firstly N₂-dewetted (600°C) and then again air-treated at 450°C lead to ~ 180 μL H₂ / 9h, i.e., the highest H₂ generation efficiency among the differently treated Pt/TiO₂ photocatalysts.

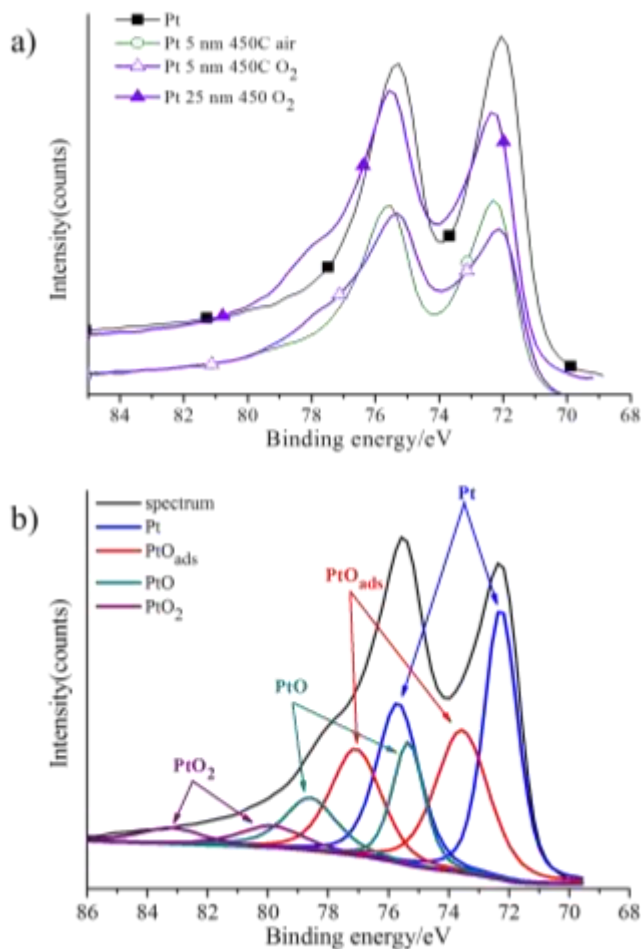


Figure 4. a) High-resolution Pt4f XPS spectrum of Pt (reference) and TiO₂ nanotube layers decorated by Pt sputter-dewetting and exposed to different thermal treatments in O₂-containing atmosphere. The Pt4f spectrum of the layer sputter-coated with a 25 nm-thick Pt film is shown in b) along with the fitting and deconvolution of contributions from PtO_{ads}, PtO and PtO₂.

Interestingly, if the sequence is inverted, i.e., Pt is dewetted (N₂/600°C) only after crystallizing the tubes in air, the H₂ evolution drops to ~ 1 μL / 9h. This is ascribed to generation of oxygen vacancies during the second annealing in reductive conditions. Such reductive defect generation is widely reported in the literature.^{36,37,44-47}

The air-crystallization step was further explored by exposing dewetted layers to air-annealing at different temperatures in the 350-550°C range. The photocatalytic results summarized in Fig. 3 (a) show that compared to an air-treatment at 450°C ($\sim 180 \mu\text{L H}_2 / 9\text{h}$), annealing at 350 and 550°C leads to rather low H_2 generation efficiencies (~ 20 and $\sim 10 \mu\text{L H}_2 / 9\text{h}$, respectively). The reasons for this become evident from the XRD data (Fig. 3 (b)). One can see that the air/350°C treatment does not induce oxide crystallization into anatase TiO_2 – only a small rutile peak is visible that may even be ascribed to the rutile formed with the previous annealing step (dewetting in N_2). Air-annealing at 550°C on the other hand leads to higher degree of crystallinity and to anatase formation, but at the same time forms a large amount of rutile.^{22,48}

This rutile formation at 550°C can be ascribed to thermal oxidation of the Ti metal substrate. In line with other works, the growth of rutile occurs firstly by rutile seeding at the metal/ TiO_2 interface and then proceeds (with higher annealing temperatures or longer thermal treatments) towards the tubes top.^{24,37,42,49} This is visible from the cross-sectional SEM images in Fig. 3 (b). Here one can see that rutile forms as a layer of some hundreds of nanometers between the tubular oxide and the Ti metal substrate. An air-treatment at 550°C leads however to a ca. 500 nm-thick rutile film, that is 2-time the thickness of that formed at 450°C.

Therefore, the absence of anatase phase in the layers air-treated at 350°C, and the predominant rutile content in the oxides crystallized at 550°C, are the reasons for the small H_2 generation yield.

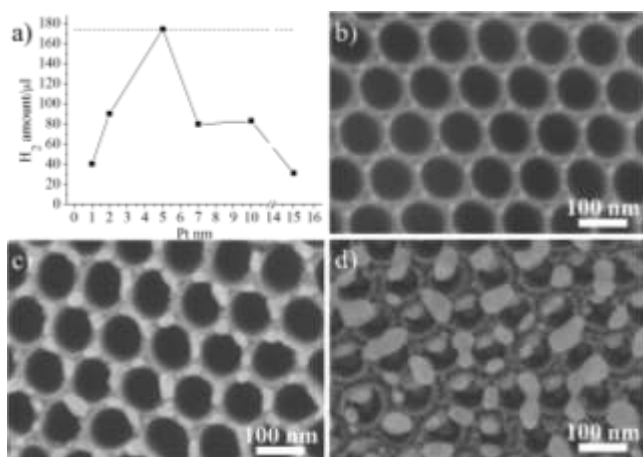


Figure 5. a) Photocatalytic H₂ generation results, and b), c), and d) SEM images of TiO₂ nanotube layers decorated by sputter-dewetting different Pt amounts, such as b) 2 nm, c) 7 nm, and d) 10 nm.

We also found that annealing in O₂-containing atmosphere can, if not properly adjusted, affect the Pt oxidation state³⁰ and therefore the co-catalyst efficiency.³² Pt/TiO₂ nanotubes annealed after dewetting in pure O₂ at 450°C produced ~ 40 μL H₂ / 9h. Please note that films treated at the same temperature in air lead instead to ~ 180 μL H₂ / 9h.

From the XPS data in Fig. 4 it can be seen that the noble metal in films air-treated at 450°C consists of metallic Pt (i.e., Pt⁰),³⁰ and the fitting of the HR spectrum in the Pt4f region shows besides the Pt⁰ signals only a small contribution (small shoulder) of adsorbed oxygen. On the contrary, for films annealed in pure O₂ an inversion of the relative intensity of the Pt4f signals is evident, and even more importantly a broad shoulder (at ~ 76-80 eV) appears that can be attributed to the formation of PtO (PtII) and PtO₂ (PtIV).³⁰

To explore more in details the possibility of Pt oxidation by O₂-annealing, Pt/tube films sputter-coated with significantly thicker Pt films (25 nm) were exposed to an identical multiple

annealing ($\text{N}_2/600^\circ\text{C}$ followed by $\text{air}/450^\circ\text{C}$). The HR XPS spectrum in Fig. 4 (a) shows an even more pronounced shoulder, and its fitting (Fig. 4 (b)) matches well with the reference Pt4f signals of PtII and PtIV oxides.^{50,51} The low H_2 generation efficiency of tube layers annealed in pure O_2 is thus ascribed to the formation of Pt oxides which deteriorates its efficiency as a co-catalyst.^{31,32, 50, 51}

In addition to the thermal treatment, we also evaluated the effect of the amount of co-catalyst on the H_2 evolution efficiency, after optimized Pt dewetting and oxide crystallization. The photocatalytic results in Fig. 5 (a) show a clear enhancement of the H_2 generation when the amount of co-catalyst is increasing up to 5 nm. Larger co-catalyst amounts, e.g., 7-15 nm-thick Pt films, showed instead a much lower photocatalytic activity.²⁶

From the SEM images in Fig. 5 (b-d) it is evident that an increase of the Pt film thickness leads to an increase of the average Pt nanoparticle size after dewetting. For Pt film of 2, 7 and 10 nm, the average Pt NPs size ranges around 5-20, 30-70 and 80-100 nm, respectively.

The smaller nanoparticles (e.g., Fig. 5 (b)) are round in shape, show a relatively narrow size distribution, and are ordered at the tubes top in hexagonal networks. Conversely, Pt islands as large as several tens of nanometers (formed from thick metal films, e.g., Fig. 5 (d)) show undefined shape and a rather broad size distribution.²⁹

The reason for the drop of photocatalytic activity observed when increasing the co-catalyst amount is therefore that while dewetting of thin Pt films exposes well the underneath oxide to the environment, thick noble metal films dewet into large Pt islands at the tube top that shade the underneath oxide and limit light absorption, this resulting in a reduced density of photo-promoted electrons. Additionally, thin metal films form Pt nanoparticles with higher specific

surface area than the large Pt islands and this enhances the area for electron transfer to the environment and therefore the H₂ evolution efficiency.

CONCLUSION

In this work we demonstrate for TiO₂ nanotubes that the quality of the oxide, in terms of crystallinity and defect density, and the morphology and chemical state of the co-catalyst (here Pt) play a crucial role in determining the photocatalytic efficiency of noble metal/TiO₂ systems. We show that a sputter-dewetting approach is a suitable technique for decorating anodic nanotube TiO₂ surfaces with fine co-catalyst nanoparticles. Even more importantly, we introduced a multiple annealing strategy by combining adequate reducing and oxidizing conditions that led to Pt dewetting and at the same time to the oxide crystallization into anatase nanotubes with reduced defect density. As a consequence, we achieved a maximized H₂ generation from such Pt/TiO₂ photocatalysts. This concept can be likely extended to other functional metal/oxide systems where the metal is even more susceptible to the annealing conditions.

ACKNOWLEDGMENT

The authors would like to acknowledge the ERC, the DFG, and the DFG “Engineering of Advanced Materials” cluster of excellence for financial support. This project was funded by the Deanship of Scientific Research (DSR), King Abdulaziz University, under grant no. 16-130-36-HiCi.

REFERENCES

- (1) Fujishima, A.; Honda, K. Electrochemical Photolysis of Water at a Semiconductor Electrode. *Nature* 1972, 238 (5358), 37–38.
- (2) Ravelli, D.; Dondi, D.; Fagnoni, M.; Albini, A. Photocatalysis. A Multi-Faceted Concept for Green Chemistry. *Chem. Soc. Rev.* 2009, 38 (7), 1999.
- (3) Hoffmann, M. R.; Martin, S. T.; Choi, W.; Bahnemann, D. W. Environmental Applications of Semiconductor Photocatalysis. *Chem. Rev.* 1995, 95 (1), 69–96.
- (4) Thompson, T. L.; Yates, J. T. Surface Science Studies of the Photoactivation of TiO₂-New Photochemical Processes. *Chem. Rev.* 2006, 106 (10), 4428–4453.
- (5) Grätzel, M. Photoelectrochemical Cells. 2001, 414, 338–344.
- (6) Paramasivam, I.; Jha, H.; Liu, N.; Schmuki, P. A Review of Photocatalysis Using Self-Organized TiO₂ Nanotubes and Other Ordered Oxide Nanostructures. *Small*. 2012, 3073–3103.
- (7) Fujishima, A.; Rao, T. N.; Tryk, D. a. Titanium Dioxide Photocatalysis. *J. Photochem. Photobiol. C Photochem. Rev.* 2000, 1 (1), 1–21.
- (8) Miao, Z.; Xu, D.; Ouyang, J.; Guo, G.; Zhao, X.; Tang, Y. Electrochemically Induced Sol-Gel Preparation of Single-Crystalline TiO₂ Nanowires. *Nano Lett.* 2002, 2 (7), 717–720.
- (9) Hagfeldt, A.; Graetzel, M. Light-Induced Redox Reactions in Nanocrystalline Systems. *Chem. Rev.* 1995, 95 (1), 49–68.

- (10) Mohapatra, S. K.; Kondamudi, N.; Banerjee, S.; Misra, M. Functionalization of Self-Organized TiO₂ Nanotubes with Pd Nanoparticles for Photocatalytic Decomposition of Dyes under Solar Light Illumination. *Langmuir* 2008, 24 (19), 11276–11281.
- (11) Su, R.; Tiruvalam, R.; Logsdail, A. J.; He, Q.; Downing, C. a; Jensen, M. T.; Dimitratos, N.; Kesavan, L.; Wells, P. P.; Bechstein, R.; et al. Designer Titania-Supported Au-Pd Nanoparticles for Efficient Photocatalytic Hydrogen Production. *ACS Nano* 2014, 8 (4), 3490–3497.
- (12) Ono, S.; Saito, M.; Asoh, H. Self-Ordering of Anodic Porous Alumina Formed in Organic Acid Electrolytes. *Electrochim. Acta* 2005, 51 (5), 827–833.
- (13) Nadeem, M. A.; Murdoch, M.; Waterhouse, G. I. N.; Metson, J. B.; Keane, M. a.; Llorca, J.; Idriss, H. Photoreaction of Ethanol on Au/TiO₂ Anatase: Comparing the Micro to Nanoparticle Size Activities of the Support for Hydrogen Production. *J. Photochem. Photobiol. A Chem.* 2010, 216 (2-3), 250–255.
- (14) Lee, K.; Hahn, R.; Altomare, M.; Selli, E.; Schmuki, P. Intrinsic Au Decoration of Growing TiO₂ Nanotubes and Formation of a High-Efficiency Photocatalyst for H₂ Production. *Adv. Mater.* 2013, 25, 6133–6137.
- (15) Chen, X.; Mao, S. S. Titanium Dioxide Nanomaterials: Synthesis, Properties, Modifications and Applications. *Chem. Rev.* 2007, 107 (7), 2891–2959.
- (16) Sugimoto, T. Preparation of Monodispersed Colloidal Particles. *Adv. Colloid Interface Sci.* 1987, 28, 65–108.

- (17) Zhang, Q.; Gao, L. Preparation of Oxide Nanocrystals with Tunable Morphologies by the Moderate Hydrothermal Method: Insights from Rutile TiO₂. *Langmuir* 2003, 19 (3), 967–971.
- (18) Liu, S. M.; Gan, L. M.; Liu, L. H.; Zhang, W. D.; Zeng, H. C. Synthesis of Single-Crystalline TiO₂ Nanotubes. *Chem. Mater.* 2002, 14 (3), 1391–1397.
- (19) Lee, K.; Mazare, A.; Schmuki, P. One-Dimensional Titanium Dioxide Nanomaterials: Nanotubes. *Chemical reviews*. 2014, 9385–9454.
- (20) Roy, P.; Berger, S.; Schmuki, P. TiO₂ Nanotubes: Synthesis and Applications. *Angew. Chemie Int. Ed.* 2011, 50 (13), 2904–2939.
- (21) Li, H.; Cheng, J.-W. W.; Shu, S.; Zhang, J.; Zheng, L.; Tsang, C. K.; Cheng, H.; Liang, F.; Lee, S.-T. T.; Li, Y. Y. Selective Removal of the Outer Shells of Anodic TiO₂ Nanotubes. *Small* 2013, 9 (1), 37–44.
- (22) Oh, H.-J.; Lee, J.-H.; Kim, Y.-J.; Suh, S.-J.; Lee, J.-H.; Chi, C.-S. Synthesis of Effective Titania Nanotubes for Wastewater Purification. *Appl. Catal. B Environ.* 2008, 84 (1-2), 142–147.
- (23) Chiarello, G. L.; Aguirre, M. H.; Selli, E. Hydrogen Production by Photocatalytic Steam Reforming of Methanol on Noble Metal-Modified TiO₂. *J. Catal.* 2010, 273 (2), 182–190.
- (24) Naldoni, A.; D'Arienzo, M.; Altomare, M.; Marelli, M.; Scotti, R.; Morazzoni, F.; Selli, E.; Dal Santo, V. Pt and Au/TiO₂ Photocatalysts for Methanol Reforming: Role of Metal Nanoparticles in Tuning Charge Trapping Properties and Photoefficiency. *Appl. Catal. B Environ.* 2013, 130-131, 239–248.

- (25) Yoo, J. E.; Lee, K.; Altomare, M.; Selli, E.; Schmuki, P. Self-Organized Arrays of Single-Metal Catalyst Particles in TiO₂ Cavities: A Highly Efficient Photocatalytic System. *Angew. Chemie Int. Ed.* 2013, 52, 1–5.
- (26) Nguyen, N. T.; Yoo, J.; Altomare, M.; Schmuki, P. “Suspended”Pt Nanoparticles over TiO₂ Nanotubes for Enhanced Photocatalytic H₂ Evolution. *Chem. Commun.* 2014, 50 (68), 9653–9656.
- (27) Yoo, J. E.; Lee, K.; Schmuki, P. Dewetted Au Films Form a Highly Active Photocatalytic System on TiO₂ Nanotube-Stumps. *Electrochem. commun.* 2013, 34, 351–355.
- (28) Nguyen, N. T.; Altomare, M.; Yoo, J.; Schmuki, P. Efficient Photocatalytic H₂ Evolution: Controlled Dewetting-Dealloying to Fabricate Site-Selective High-Activity Nanoporous Au Particles on Highly Ordered TiO₂ Nanotube Arrays. *Adv. Mater.* 2015, 27, 3208–3215.
- (29) Thompson, C. V. Solid-State Dewetting of Thin Films. *Annu. Rev. Mater. Res.* 2012, 42 (1), 399–434.
- (30) Lee, J.; Choi, W. Photocatalytic Reactivity of Surface Platinized TiO₂: Substrate Specificity and the Effect of Pt Oxidation State. *J. Phys. Chem. B* 2005, 109 (15), 7399–7406.
- (31) Teoh, W. Y.; Mädler, L.; Amal, R. Inter-Relationship between Pt Oxidation States on TiO₂ and the Photocatalytic Mineralisation of Organic Matters. *J. Catal.* 2007, 251, 271–280.
- (32) Chiarello, G. L.; Dozzi, M. V.; Scavini, M.; Grunwaldt, J.-D.; Selli, E. One Step Flame-Made Fluorinated Pt/TiO₂ Photocatalysts for Hydrogen Production. *Appl. Catal. B Environ.* 2014, 160-161, 144–151.

- (33) Ghicov, A.; Macak, J. M.; Tsuchiya, H.; Kunze, J.; Haeublein, V.; Frey, L.; Schmuki, P. Ion Implantation and Annealing for an Efficient N-Doping of TiO₂ Nanotubes. *Nano Lett.* 2006, 6 (5), 1080–1082.
- (34) Fox, M. A.; Dulay, M. T. Heterogeneous Photocatalysis. *Chem. Rev.* 1993, 93 (1), 341–357.
- (35) Chiarello, G. L.; Ferri, D.; Selli, E. Effect of the CH₃OH/H₂O Ratio on the Mechanism of the Gas-Phase Photocatalytic Reforming of Methanol on Noble Metal-Modified TiO₂. *J. Catal.* 2011, 280 (2), 168–177.
- (36) Nguyen, N. T.; Altomare, M.; Yoo, J. E.; Taccardi, N.; Schmuki, P. Noble Metals on Anodic TiO₂ Nanotube Mouths: Thermal Dewetting of Minimal Pt Co-Catalyst Loading Leads to Significantly Enhanced Photocatalytic H₂ Generation. *Adv. Energy Mater.* 2015.
- (37) Zhu, K.; Neale, N. R.; Halverson, A. F.; Kim, J. Y.; Frank, A. J. Effects of Annealing Temperature on the Charge-Collection and Light-Harvesting Properties of TiO₂ Nanotube-Based Dye-Sensitized Solar Cells. *J. Phys. Chem. C* 2010, 114 (32), 13433–13441.
- (38) Altomare, M.; Pozzi, M.; Allieta, M.; Bettini, L. G.; Selli, E. H₂ and O₂ Photocatalytic Production on TiO₂ Nanotube Arrays: Effect of the Anodization Time on Structural Features and Photoactivity. *Appl. Catal. B Environ.* 2013, 136-137, 81–88.
- (39) Ozkan, S.; Mazare, A.; Schmuki, P. Extracting the Limiting Factors in Photocurrent Measurements on TiO₂ Nanotubes and Enhancing the Photoelectrochemical Properties by Nb Doping. *Electrochim. Acta* 2015, 176, 819–826.

- (40) Mohammadpour, F.; Moradi, M.; Lee, K.; Cha, G.; So, S.; Kahnt, A.; Guldi, D. M.; Altomare, M.; Schmuki, P. Enhanced Performance of Dye-Sensitized Solar Cells Based on TiO₂ Nanotube Membranes Using an Optimized Annealing Profile. *Chem. Commun.* 2015, 51 (9), 1631–1634.
- (41) Liu, F.; Lu, L.; Xiao, P.; He, H.; Qiao, L.; Zhang, Y. Effect of Oxygen Vacancies on Photocatalytic Efficiency of TiO₂ Nanotubes Aggregation. *Bull. Korean Chem. Soc.* 2012, 33 (7), 2255–2259.
- (42) Albu, S. P.; Tsuchiya, H.; Fujimoto, S.; Schmuki, P. TiO₂ Nanotubes - Annealing Effects on Detailed Morphology and Structure. *Eur. J. Inorg. Chem.* 2010, 4351–4356.
- (43) Ghicov, A.; Albu, S. P.; Hahn, R.; Kim, D.; Stergiopoulos, T.; Kunze, J.; Schiller, C. A.; Falaras, P.; Schmuki, P. TiO₂ Nanotubes in Dye-Sensitized Solar Cells: Critical Factors for the Conversion Efficiency. *Chem. - An Asian J.* 2009, 4 (4), 520–525.
- (44) Naldoni, A.; Fabbri, F.; Altomare, M.; Marelli, M.; Psaro, R.; Selli, E.; Salviati, G.; Dal Santo, V. The Critical Role of Intragap States in the Energy Transfer from Gold Nanoparticles to TiO₂. *Phys. Chem. Chem. Phys.* 2015, 17 (7), 4864–4869.
- (45) Naldoni, A.; Allieta, M.; Santangelo, S.; Marelli, M.; Fabbri, F.; Cappelli, S.; Bianchi, C. L.; Psaro, R.; Dal Santo, V. Effect of Nature and Location of Defects on Bandgap Narrowing in Black TiO₂ Nanoparticles. *J. Am. Chem. Soc.* 2012, 134 (18), 7600–7603.
- (46) Chen, X.; Liu, L.; Yu, P. Y.; Mao, S. S. Increasing Solar Absorption for Photocatalysis with Black Hydrogenated Titanium Dioxide Nanocrystals. *Science* 2011, 331 (6018), 746–750.

- (47) Liu, N.; Schneider, C.; Freitag, D.; Hartmann, M.; Venkatesan, U.; Müller, J.; Spiecker, E.; Schmuki, P. Black TiO₂ Nanotubes: Cocatalyst-Free Open-Circuit Hydrogen Generation. *Nano Lett.* 2014, 14 (6), 3309–3313.
- (48) Macak, J. M.; Zlamal, M.; Krysa, J.; Schmuki, P. Self-Organized TiO₂ Nanotube Layers as Highly Efficient Photocatalysts. *Small* 2007, 3 (2), 300–304.
- (49) Selli, E.; Chiarello, G. L.; Quartarone, E.; Mustarelli, P.; Rossetti, I.; Forni, L. A Photocatalytic Water Splitting Device for Separate Hydrogen and Oxygen Evolution. *Chem. Commun.* 2007, 47, 5022.
- (50) Kim, K. S.; Winograd, N.; Davis, R. E. Electron Spectroscopy of Platinum-Oxygen Surfaces and Application to Electrochemical Studies. *J. Am. Chem. Soc.* 1971, 93 (23), 6296–6297.
- (51) Scott, J.; Irawaty, W.; Low, G.; Amal, R. Enhancing the Catalytic Oxidation Capacity of Pt/TiO₂ Using a Light Pre-Treatment Approach. *Appl. Catal. B Environ.* 2015, 164, 10–17.

